VERSITA

Conduction in nanostructured La$_{1-x}$Sr$_x$FeO$_3$ (0 ≤ x ≤ 1)

A. ZAFAR[1], Z. IMRAN[1], M.A. RAFIQ[1*], S. H. SHAH[2], M.M. HASAN[1]

[1]Micro and Nano Devices Group, Department of Metallurgy and Materials Engineering,
Pakistan Institute of Engineering and Applied Sciences, P.O. Nilore, Islamabad, 45650, Pakistan

[2]TPPD, PINSTECH, P.O. Nilore, Islamabad, 45650, Pakistan

We investigated electrical properties of nanostructured La$_{1-x}$Sr$_x$FeO$_3$ (0 ≤ x ≤ 1) from 300 K – 400 K. The nanostructured La$_{1-x}$Sr$_x$FeO$_3$ (0 ≤ x ≤ 1) was synthesized by citrate gel method requiring no pH control. X-ray diffraction pattern showed that single phase LaFeO$_3$ with an orthorhombic structure was formed. The structure changed into rhombohedral for x = 0.5 and it became cubic for x = 1.0. For x ≤ 0.5, our material showed non-linear current-voltage characteristics and for x > 0.5 it showed linear current-voltage characteristics. Poole Frenkel type conduction mechanism was found to be operative in LaFeO$_3$ from 300 K – 400 K. The experimental values of field-lowering coefficient were by 2.56-6.41 times higher than the predicted value and were attributed to the presence of localized fields. The increase in conductance with Sr content was due to formation of Fe^{4+} ions in addition to Fe^{3+} with the increase in Sr content. Impedance spectroscopy and ac conductivity analysis of La$_{1-x}$Sr$_x$FeO$_3$ (0 ≤ x ≤ 1) was also carried out in the temperature range from 300 K – 400 K and frequency was varied from 20 Hz – 2 MHz. The ac conduction followed the correlated barrier hopping model in La$_{0.9}$Sr$_{0.1}$FeO$_3$.

Keywords: *electrical properties, conduction, oxides, chemical synthesis*

1. Introduction

In recent years there has been a great interest in perovskite type oxides due to their unique properties [1, 2]. These oxides have a general formula, *ABO*$_3$, where *A* and *B* are usually rare earth and transition metal cations respectively. These oxides have versatile physical properties such as magnetoresistance [3], superconductivity [4] and ferroelectricity [5].

One of the most common perovskite oxides, LaFeO$_3$, is a p-type semiconductor material [6]. It is an antiferromagnetic material at room temperature [7]. The perovskite series La$_{1-x}$Sr$_x$FeO$_3$ (0 ≤ x ≤ 1) and parent material LaFeO$_3$ have been studied extensively due to their vast applications. The perovskite series can be used as sensors [8, 9], catalysts [10, 11] and fuel cells [12]. The La$_{1-x}$Sr$_x$FeO$_3$ series may also be used as semiconductors, thermistors and capacitors [13].

The understanding of the transport properties of these materials is very important for right choice of their applications. Bongio et al. [14] investigated four probe dc electrical conductivity of La$_{1-x}$Sr$_x$FeO$_3$ (x = 0.2 - 0.9). They concluded that the maximum conductivity for La$_{0.5}$Sr$_{0.5}$FeO$_3$ sintered in flowing air at 1400 °C was 352 S/cm at 550 °C. Jung et al. [7] investigated ac and dc conductivity of La$_{1-x}$Sr$_x$FeO$_3$ (0.05 ≤ x ≤ 0.3). Electrical conductivity of La$_{1-x}$Sr$_x$FeO$_3$ (x = 0.2, 0.4, 0.5, 0.7, 0.9) has also been analyzed over a wide range of oxygen partial pressures [15].

However, there has been more emphasis on ac conductivity and impedance spectroscopy of the above mentioned perovskite series. There are not many studies of dc conduction mechanism in the perovskite series La$_{1-x}$Sr$_x$FeO$_3$ (0 ≤ x ≤ 1) and the parent material LaFeO$_3$. In this paper we investigated dc conduction in these materials from 300 K – 400 K. The nanostructured La$_{1-x}$Sr$_x$FeO$_3$ (0 ≤ x ≤ 1) was synthesized by citrate gel technique. The phase purity and particle size were determined using X-ray diffraction (XRD) and scanning electron microscope. As the Sr content increased, an increase in conductance

———————
*E-mail: fac221@pieas.edu.pk

was observed. Poole-Frenkel type conduction mechanism was found to be operative in LaFeO$_3$. We have also investigated ac electrical properties of the system. The ac electrical measurements were performed using an Agilent E4980A LCR meter from 300 K – 400 K. The frequency of the ac signal was varied from 20 Hz – 2 MHz.
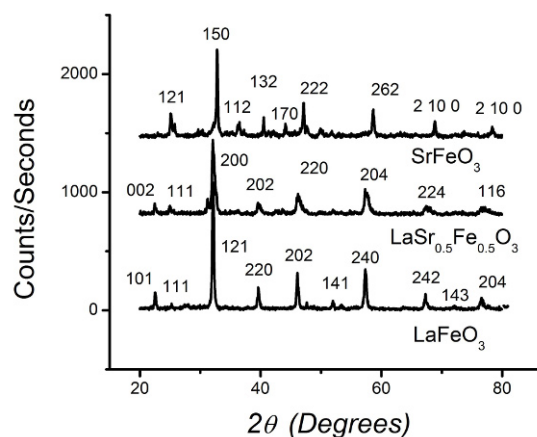
2. Materials and Methods

Nanostructured La$_{1-x}$Sr$_x$FeO$_3$ (0 ≤ x ≤ 1) was prepared by citrate gel method. The method is relatively simple and does not require pH control, vacuum or high temperature. The chemical interaction between the material and the container is negligible in this method. Stoichiometric amounts of La (NO$_3$)$_3$·6H$_2$O, Fe (NO$_3$)$_3$·9H$_2$O and Sr (NO$_3$)$_2$ were taken and the solutions in distilled water were prepared. These solutions were then poured dropwise into citric acid which acted as a chelating agent. The resulting solution was stirred continuously while keeping the temperature of the solution between 70 – 80 °C. Initially, a sol was formed. The sol was then gradually converted into a reddish brown gel complex. The gel was dried and combusted, until powder was obtained. After grounding and heating at 300 °C for 3 hours followed by grinding and heating at 450 °C for 3 hours, the powder was again ground and heated at 600 °C for 3 hours followed by grinding and heating at 800 °C for 3 hours. The powder was pressed into cylindrical pellets of 10 mm diameter by uniaxial pressure in a hydraulic press at 6 tons load. The green pellets were sintered at 800 °C for 3 hours. A heating rate of 5 °C/min. was used to reach the temperature.
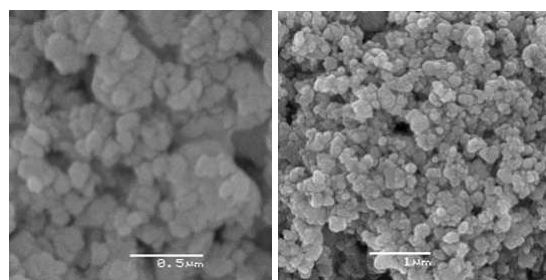
Electrical contacts were made with silver paste on both sides of the pellets. Dc electrical measurements were performed in vacuum on each sample using Keithley 2400 source-meter from 300 K – 400 K.

3. Results and Discussion

Fig. 1(a) shows the XRD patterns of nanostructured La$_{1-x}$Sr$_x$FeO$_3$ (x = 0, 0.5, 1)

(a)

(b)   (c)

Fig. 1. (a) XRD patterns of nanostructured LaFeO$_3$, La$_{0.5}$Sr$_{0.5}$FeO$_3$ and SrFeO$_3$ (b) SEM image of nanostructured LaFeO$_3$ (c) SEM image of nanostructured La$_{0.9}$Sr$_{0.1}$FeO$_3$.

using the Bruker D8 Discover Diffractometer equipped with CuKα radiation. The observed XRD pattern shows the formation of single phase LaFeO$_3$ with an orthorhombic structure and it matches with JCPDS card No 37-1493. The calculated lattice parameters (a = 0.55560 nm, b = 0.7864 nm and c = 0.5567 nm) are consistent with the reported results [16]. As the Sr content increases, the structure changes to rhombohedral and becomes cubic when La is completely replaced by Sr. The XRD patterns of La$_{0.5}$Sr$_{0.5}$FeO$_{0.5}$ and SrFeO$_3$ match with JCPDS card No 82-1959 and 71-1975 respectively. The calculated lattice parameters for SrFeO$_3$ (a = b = c = 0.385 nm) are consistent with the reported results [17].

Fig. 1(b) and 1(c) show the scanning electron micrographs of nanostructured LaFeO$_3$ and

$La_{0.9}Sr_{0.1}FeO_3$ respectively, obtained using JSM-5910 JEOL, Japan. The micrographs show that the material is composed of nano-size crystallites. The average crystallite size was found to be ∼50 nm for $LaFeO_3$ and ∼80 nm for $La_{0.9}Sr_{0.1}FeO_3$.

Fig. 2(a) and (b) show the current-voltage (I-V) characteristics of $LaFeO_3$ and $La_{0.3}Sr_{0.7}FeO_3$ respectively from 300 K – 400 K. The I-V characteristics are nonlinear for $LaFeO_3$. Similar behavior is observed for x = 0.1, 0.3 and 0.5 (not shown) as well. However the I-V curves become linear and the magnitude of the current increases for x = 0.7, 0.9 and 1 (I-V curves for x = 0.9 and 1 are not shown). The non-linear behavior in the I-V characteristics for x = 0 - 0.5 shows that our samples have non-ohmic character. For x = 0.7 - 1.0, our samples have ohmic character.

We considered various possible conduction mechanisms for our Sr doped lanthanum ferrite samples. However, Poole-Frenkel type of conduction mechanism explains the I-V characteristics of our samples. Schottky type conduction also follows similar electric field dependence. However, the I-V characteristics of all samples are highly symmetric and we think that Schottky type behavior may not be possible in our case.

In case of Poole-Frankel conduction mechanism, the current density is given by [18]:
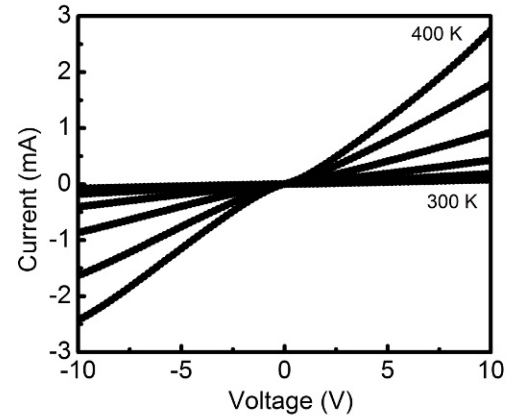
$$J = \sigma_0 E \exp\left[\frac{\beta E^{1/2}}{kT}\right] \quad (1)$$

Here, σ_0 is a low field conductivity, k is Boltzmann constant, T is the measurement temperature and E is an average electric field. The Poole-Frenkel field lowering coefficient β is given by:
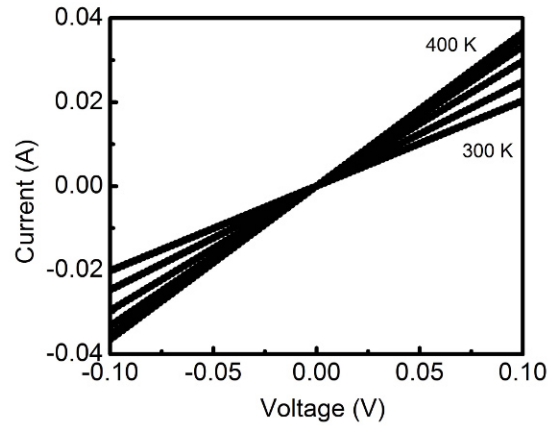
$$\beta = \left(\frac{e^3}{\pi \varepsilon_r \varepsilon_0}\right)^{1/2} \quad (2)$$

where ε_r is the relative dielectric constant, ε_0 is permittivity of free space and e is electronic charge.

Fig. 3 shows the variation of $\ln J/E$ with square root of E. It is obvious that the conduction in

(a)

(b)

Fig. 2. I-V characteristics of (a) nanostructured $LaFeO_3$ (b) nanostructured $La_{0.3}Sr_{0.7}FeO_3$ from 300 K – 400 K with temperature step of 20 K.

$LaFeO_3$ at higher fields follows the dependence given by Equation 1. From the slopes of the curves in Fig. 3, the experimental value of field lowering coefficient β was determined. The theoretical value of β obtained from Equation 2 and is 0.407×10^{-4} eV $V^{-1/2}$ $m^{1/2}$. Here, we used the value of dielectric constant $\varepsilon_r = 3.4596 \pm 0.0054$. The value was taken from the refractive index n ($\varepsilon_r = n^2$) of $LaFeO_3$ annealed at 800 °C [19]. In our samples the maximum annealing temperature was 800 °C as well. The experimental values of β obtained on the basis of Fig. 2 are listed in Table 1. The experimental values of β for $LaFeO_3$ are by
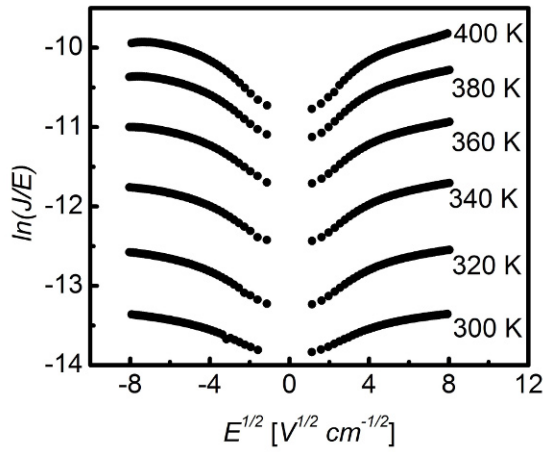
Fig. 3. ln J/E vs. square root of applied electric field for nanostructured LaFeO$_3$ at various temperatures.

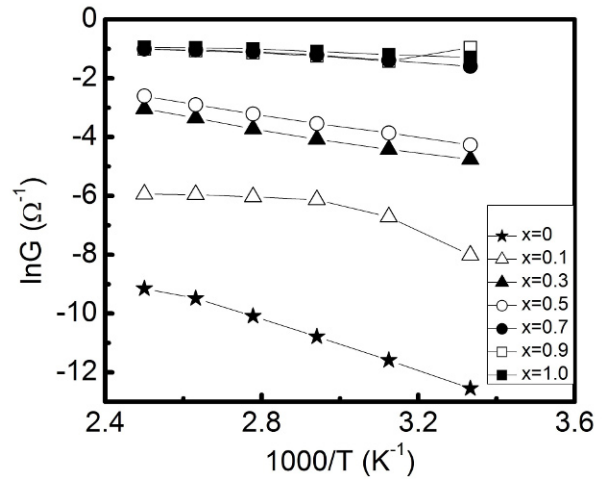Table 1. Experimental values of β at different temperatures for LaFeO$_3$.

Temperature (K)	β (eV V$^{-1/2}$ m$^{1/2}$)
300	1.003×10^{-4}
320	1.378×10^{-4}
340	1.582×10^{-4}
360	1.768×10^{-4}
380	2.060×10^{-4}
400	2.561×10^{-4}

2.5-6.4 times higher than the theoretical value of β. The higher experimental values of β can be explained by the existence of localized electric fields within the sample. The localized fields have the values greater than the mean field E [18]. In this case Poole-Frenkel conductivity is given by:
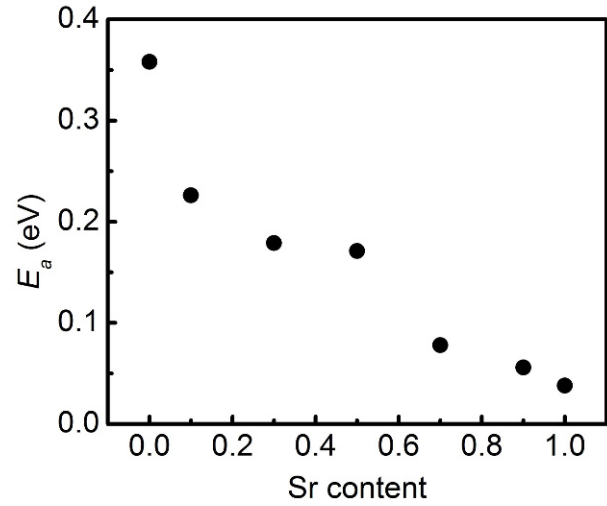
$$J = \frac{2J_0 kT}{\alpha \beta F^{1/2}} \exp\left(\frac{\beta E^{1/2}}{kT}\right) \qquad (3)$$

Here, the maximum internal electric field is $\alpha^2 E$ whereas α^2 is a field enhancement coefficient. The field enhancement coefficient α is the ratio of experimental value of β to the theoretical value of β. Therefore, for LaFeO$_3$ α has values in the range of $2.5 - 6.4$ and in consequence, the field enhancement coefficient α^2 has the values in the range of $6.25 - 40.96$.

Fig. 4(a) shows the variation of conductance versus inverse of temperature at $V = 0.1$ V for the

(a)

(b)

Fig. 4. (a) Temperature dependence of conductance of nanostructured La$_{1-x}$Sr$_x$FeO$_3$ (0 ≤ x ≤ 1) at $V = 0.1$ V (b) Variation of activation energy of nanostructured La$_{1-x}$Sr$_x$FeO$_3$ (0 ≤ x ≤ 1) with Sr content.

nanostructured La$_{1-x}$Sr$_x$FeO$_3$ (0 ≤ x ≤ 1). The conductance increases as the Sr content increases. However for x ≥ 0.7, the increase in conductance is very small. Activation energies, calculated from Fig. 4(a), are plotted in Fig. 4(b). The activation energy decreases as the Sr content increases due to the lowering of the potential barrier for the conduction. The calculated activation energies lie in the range of 0.035-0.4 eV.

The observed increase in conductance with Sr content can be explained as follows.

$LaFeO_3$ has $3d^5$ ground state and is in high spin configuration [20]. The six oxygen anions approach the metal cation and split its 3d level to remove degeneracy. Replacement of La^{3+} by Sr^{2+} leads to the decrease in the cell volume (decrease in the cell volume is clear from XRD data) and decrease in the bond length of Fe-O. For the compensation and charge neutrality, Fe^{4+} ions are formed [21]. Therefore, in the samples doped with Sr, there are also cations of Fe with different valances i.e. Fe^{3+} and Fe^{4+}. According to Verwey et al. [22], the presence of cations of the same element but with oxidation numbers differing by unity leads to higher electrical conductivity in transition element oxides. Such cations should be at similar sites in the crystal structure. In present case, therefore, we suggest that the formation of Fe^{4+} ions in addition to Fe^{3+} ions with increase in Sr content is responsible for the observed increase in electrical conductance.

Impedance measurements were performed in the frequency range of 20 Hz – 2 MHz using an Agilent E4980A LCR meter. The temperature range was 300 K – 400 K with a temperature step of 10 K. Fig. 5(a) shows the Nyquist plot for $La_{0.9}Sr_{0.1}FeO_3$ from 300 K – 400 K. A single semicircular arc is observed for x = 0.1 and 0.3 (not shown), while a nearly linear response was observed for x ≥ 0.5. Fig. 5(a) shows that as the temperature increases, the resistance of the $La_{0.9}Sr_{0.1}FeO_3$ decreases. Fig. 5(b) shows the variation of the imaginary part of the impedance (Z'') with frequency. A single peak is observed at x = 0.1 and 0.3 (not shown) plots. The value of the peak maximum (Z''_{max}) decreases and the peak broadens as the temperature rises. At the same time the peak maximum shifts towards higher values of frequency. These facts indicate accumulation of space charge in the sample [23].

Relaxation time τ has been calculated from the following equation:

$$\tau = \frac{1}{2\pi f_{max}} \tag{4}$$

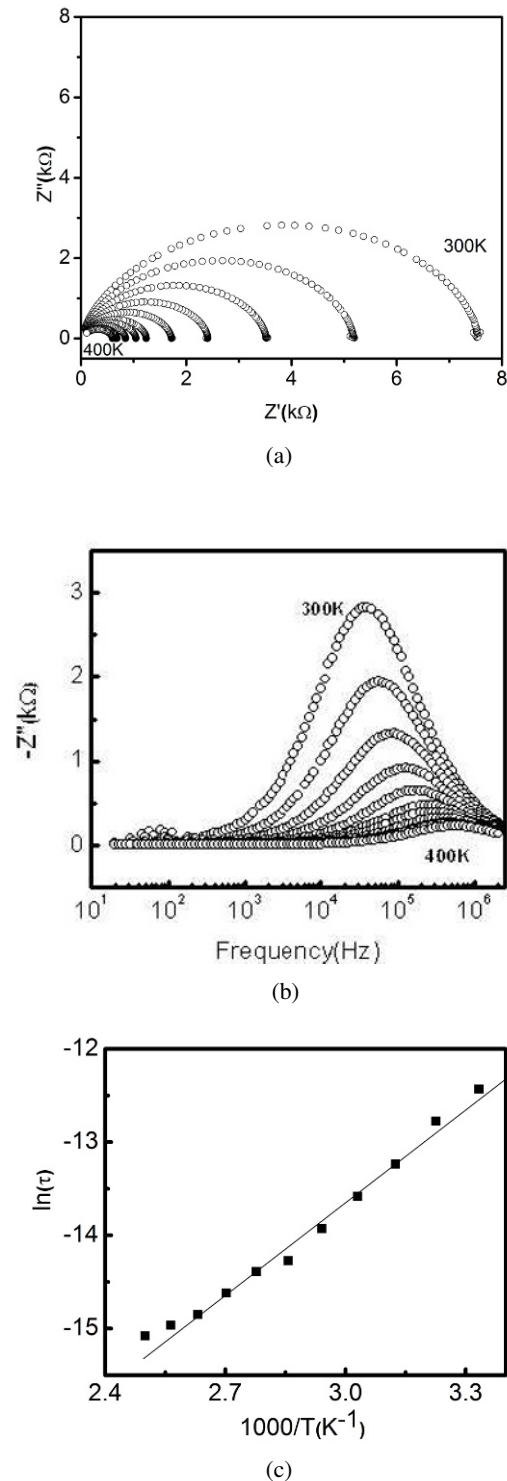Where f_{max} is the frequency at Z_{max}. The variation in $\ln(\tau)$ with inverse of temperature

(a)

(b)

(c)

Fig. 5. (a) Nyquist plot (b) frequency dependence of Z'' (c) temperature dependence of relaxation time for $La_{0.9}Sr_{0.1}FeO_3$ from 300 K – 400 K.

is plotted in Fig. 5(c). It may be noted that the relaxation time increases with increase in temperature for La$_{0.9}$Sr$_{0.1}$FeO$_3$. The activation energies are calculated from the slope of ln(τ) vs 1/T curve. The calculated activation energy for La$_{0.9}$Sr$_{0.1}$FeO$_3$ is 0.28 eV.

Ac conductivity of the pellet was investigated in the frequency range of 20 Hz – 2 MHz and at temperatures from 300 K - 400 K. The ac conductivity variation with frequency is given by [23]

$$\sigma_{ac} = A\omega^s \qquad (5)$$

where ω is the angular frequency, A is a constant and the exponent 's' is a material property which can take any value between 0 and 1.

Fig. 6(a) shows the frequency dependence of ac conductivity of La$_{0.9}$Sr$_{0.1}$FeO$_3$. It is clearly seen that there are two distinct regions: region 1 which is almost frequency independent and region 2 which is strongly frequency dependent. The values of the exponent '*s*' were determined from Fig. 6(a) at different temperatures and are shown in Fig. 6(b). The exponent 's' decreases with temperature indicating the correlated barrier hopping mechanism. Using this model [23] the binding energy can be calculated using the expression:

$$S = 1 - \beta \qquad (6)$$

where

$$\beta = \frac{6Tk_B}{W_m} \qquad (7)$$

where W_m is the binding energy, which is the energy needed to remove an electron completely and transfer it from one site to another. Fig. 7(a) shows the decrease in binding energy with the rise of temperature.

By using the values of the binding energy, minimum hopping distance R_{min} is calculated by [6].

$$R_{min} = \frac{2e^2}{W_m \pi \varepsilon \varepsilon_0} \qquad (8)$$

where ε is the dielectric constant and ε_0 is the permittivity of free space. Fig. 7(b) shows the

(a)

(b)
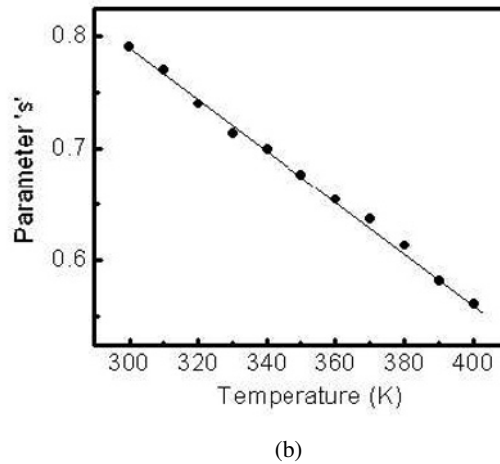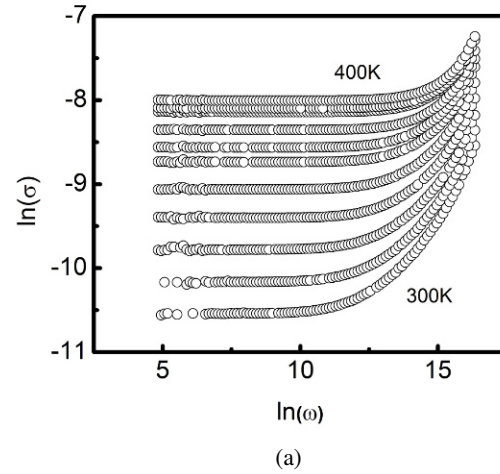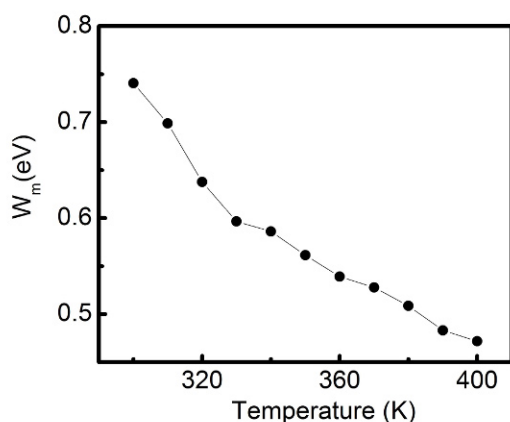
Fig. 6. (a) Frequency dependence of ac conductivity of nanostructured La$_{0.9}$Sr$_{0.1}$FeO$_3$ from 300 K – 400 K with temperature step of 10 K (b) variation of *s* with temperature.

variation of minimum hopping distance (R_{min}) with temperature at 10^4 Hz.
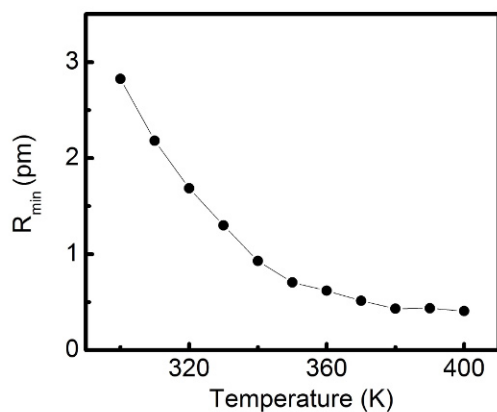
Fig. 8 shows the variation in the ac conductivity with the reciprocal of temperature at different compositions. The ac conductivity increases with increase in Sr content.

4. Conclusions

We prepared nanostructured La$_{1-x}$Sr$_x$FeO$_3$ (0 ≤ x ≤ 1) by citrate gel method. XRD confirmed that LaFeO$_3$, La$_{0.5}$Sr$_{0.5}$FeO$_3$ and SrFeO$_3$ had

(a)

(b)

Fig. 7. (a) Variation of binding energy W_m with temperature (b) variation of minimum hoping distance with temperature.

orthorhombic, rhombohedral and cubic structure respectively. For x $\leq$ 0.5 the *I-V* characteristics of our material were non-linear and for x > 0.5 the *I-V* characteristics were linear. Further, with increase in the Sr content, the conductance of our samples increased. This increase in conductance was attributed to the formation of Fe^{4+} ions in addition to Fe^{3+} ions as Sr content increased. Poole-Frenkel type conduction mechanism was found be operative in $LaFeO_3$ from 300 K – 400 K. Impedance spectroscopy and conductivity analysis of $La_{1-x}Sr_xFeO_3$ (0 $\leq$ x $\leq$ 1) was carried out in the temperature range of 300 K – 400 K and
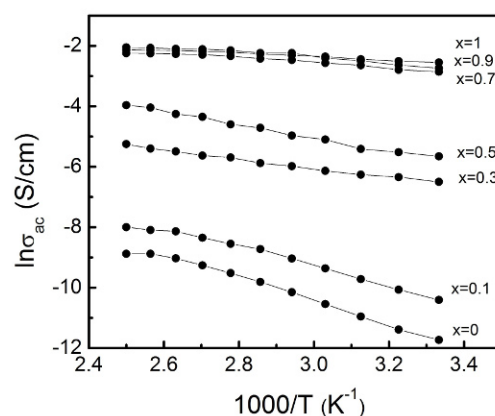

Fig. 8. Variation in ac conductivity with temperature as a function of composition at 20 kHz.

frequency range of 20 Hz – 2 MHz. It has been found the conduction mechanism in $La_{0.9}Sr_{0.1}FeO_3$ is controlled by correlated barrier hopping.

References

[1] VON HELMOLT R., WECKER J., HOLZAPFEL B., SCHULTZ L., SAMWER K., *Phys. Rev. Lett.* 71 (1993) 2331.

[2] RAO C. N. R., RAVEAU B., Colossal Magnetoresistance, Charge Ordering, and Related Properties of Manganese Oxides, World Scientific, Singapore, 1998.

[3] MAAT S., CAREY M. J., FULLERTON E. E., LE T. X., RICE P. M., GURNEY B. A., *Appl. Phys. Lett.* 81, (2002) 520.

[4] TARASCON J. M., GREENE L. H., MCKINNON W. R., HULL G. W., GEBALLE T. H., *Science* 235 (4794) (1987) 1373.

[5] BASANTAKUMAR H. S., SARMA H. N. K., MANSINGH A., *J. Mater. Sci.*, 34 (1999) 1385.

[6] ELISABETTA D. B., LUISA G. M., YOON J. W., ENRICO T., *J. Americ. Cer. Soc.* 87 (2004) 1883

[7] JUNG W. H., IGUCHI E., *J. Phys: Condens. Mat.*, 7 (1995) 1215.

[8] TOAN N. N., SAUKKOAND S., LANTTO V., *Physica B: Condensed Matter*, 327 (2003) 279.

[9] MURADE P. A., SANGAWAR V. S., CHAUDHARI G.N., KAPSE V.D., BAJPEYEE A.U., *Curr. Appl. Phys.* 11 (2011) 451.

[10] BAI S. L., SHI B. J., MA L. J., YANG P. C., LIU Z. Y., LI D. Q., CHEN A. F., *Science China Series B: Chemistry*, 52 (2009) 2106.

[11] ZHONG H., ZENG R., *Serb J. Chem. Soc.* 71 (2006) 1049.

[12] MIZUSAKI J., SASAMOTO T., CANNON W. R.,

BOWEN H. K., *J. Am. Ceram.Soc.*, 66 (1983) 247.

[13] LI J., KOU X., QIN Y., HE H., *Phys. Status. Solidi. (a)* 191 (2002) 255.

[14] BONGIO E. V., BLACK H., RASZEWSKI F. C., EDWARDS D., MCCONVILLE C. J., AMARAKOON V. R. W., *J. Electroceram.*, 14 (2005) 193.

[15] PATRAKEEV M. V., BAHTEEVA J. A., MITBERG E. B., LEONIDV I. A., KOZHEVINIKOV V. L., POEPPELMEIER K. R., *J. Solid State Chem.*, 172 (2003) 219.

[16] ZHENG W., LIU R., PENG D., MENG G., *Mater. Lett.* 43 (2000) 19.

[17] AUGSTIN C. O., SELVAN R. K., NAGARAJ. R., BERCHMANS L. J., *Mater. Chem. and phys.* 89 (2005) 406.

[18] GOULD R. D., BOWLER C. J., *Thin Solid Films* 164 (1988) 281.

[19] RAJENDRAN M., KRISHNA M. G., BHATACHARYA A. K., *Modern Physics Letters B*, 14 (2000) 801.

[20] IGUCHI E., JUNG W. H., *J. Phys. Soc. Japan* 63 (1994) 3078.

[21] VOGT U. F., SFEIR J., RICHTER J., SOLTMANN C., HOLTAPPELS P., *Pure Appl. Chem.*, 80 (2008) 2543.

[22] VERWEY E. J. W., HAAIJMAN P. W., ROMEYN F. C., OOSTERHOUT G. W., *Philips Rev. Rep.* 9 (1947) 239.

[23] LILY, KUMARI K., PRASAD K., CHOUDHRY R. N. P., *J. Alloy. Compd.* 453 (2008) 325.